Science and Technology Infusion Climate Bulletin
NOAA's National Weather Service
42nd NOAA Annual Climate Diagnostics and Prediction Workshop
Norman, OK, 23-26 October 2017

An Overview of the 2016-17 La Niña and Return to Neutral Conditions

Michelle L'Heureux
[1]*Climate Prediction Center, NOAA/NWS/NCEP, College Park, MD*

1. ENSO evolution and forecasts during 2016-17

A very brief and weak La Niña followed the major El Niño of 2015-16. NOAA Climate Prediction Center (CPC) issued its first La Niña Watch in April 2016, during the decay of the major El Niño of 2015-16 (L'Heureux *et al.*, 2017). At that time, most model forecasts were strongly anticipating a transition to a moderate La Niña by Northern Hemisphere summer 2016 (Niño-3.4 index values between -1°C and -1.4°C). The grey lines in Fig. 1 show that ensemble mean forecasts of Niño-3.4 from the North American Multi-Model Ensemble (NMME), initialized in early-mid 2016, were much colder than what actually occurred (black line). That most ensemble members from the NMME were too cold was reflected in the very negative Log Skill Scores (LSS) for almost all forecast leads for the target month of July 2016 (Fig. 2- top and middle panels).

By August 2016, sea surface temperature (SST) anomalies in the Niño-3.4 region (5°S-5°N, 120°W-170°W) decreased to near -0.5°C. By then the models were forecasting borderline La Niña or ENSO-neutral conditions for the upcoming fall and winter, so there was much uncertainty whether the period would qualify as a historical La Niña episode as classified by NOAA (requiring 5 consecutive 3-month overlapping seasons at or less than -0.5°C in the Niño-3.4 index). As a result, a La Niña Advisory was not issued until early November 2016 when it became more certain that the event would last long enough to meet NOAA's criteria.

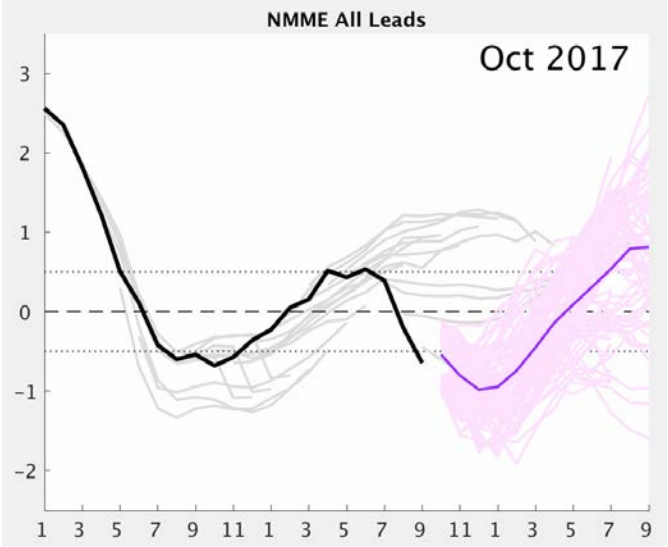

Fig. 1 Observed monthly Niño-3.4 index values (black line) from daily OISST (Reynolds *et al.* 2007) and once monthly forecasts of Niño-3.4 from the North American Multi-Model (NMME) from January 2016 through October 2017 (grey lines showing ensemble means). The pink and purple lines show the NMME forecast ensemble initialized in October 2017. The x-axis shows the month and the y-axis shows the Niño-3.4 index value. Departures are formed by removing monthly means during 1982-2010.

Not only did the NMME predict too cold conditions in Niño-3.4 during the summer of 2016, but for runs made in mid-to-late 2016, the majority of model members were also indicating too cold conditions for early 2017. Figure 2 (bottom panel) shows that NMME forecasts of Niño-3.4 had a negative bias for April 2017, particularly at longer forecast leads. While the individual forecast members are not displayed for other target months, this bias occurred at longer leads for targets during January-March 2017 as well (Fig. 2- top panel). Thus, the majority of models were anticipating La Niña to last longer than it did, abruptly ending by January 2017 and returning to ENSO-neutral.

In retrospect, the 2016-17 La Niña ended up as one of the weakest and shortest episodes in the ERSSTv5 data (Huang *et al.*, 2017) extending back to 1950, lasting exactly five consecutive seasons from July-

Correspondence to: Michelle L'Heureux, Climate Prediction Center, NOAA/NWS/NCEP, College Park, MD 20740;
E-mail: michelle.lheureux@noaa.gov

September (JAS) 2016 – November-January (NDJ) 2016-17 (with a maximum amplitude of -0.7°C). Notably, the La Niña of 2016-17 was so marginal that the Bureau of Meteorology in Australia never reached its own La Niña thresholds, meaning it is debatable whether the 2016-17 La Niña was robust enough to be considered a full-blown event.

2. Global temperature, precipitation, and circulation anomalies during NDJ 2016-17 and their relation with ENSO

CPC defines the Northern Hemisphere winter season as the December-January (DJF) average, but because La Niña officially only lasted through NDJ 2016-17 (see previous section), the analysis in this section is only presented for NDJ. The left column of Fig. 3 shows observed climate anomalies during NDJ 2016-17 and the right column shows the regression of these climate anomalies onto the Niño-3.4 index, which helps to diagnose the anomalies linearly associated with ENSO (note: there are also non-linear anomalies, but these are not presented herein). The regression patterns presented in the right column are multiplied by a factor and multiplied by minus one, so that the La Niña anomalies can be seen more clearly and compared with the observations. In the top right corner of each row, the spatial correlation (with the spatial mean removed) between the observations and the ENSO regression is displayed for 500-hPa geopotential height and winds (top row), surface temperature (middle row), and precipitation (bottom row).

Among all the variables, the largest spatial correlation (r=-0.42) or match between the observed anomalies and the expected linear ENSO pattern occurs for precipitation (Fig. 3, bottom row). Corresponding to La Niña, NDJ 2016-17 precipitation was enhanced over the Maritime Continent and Southeast Asia, northwestern Australia, over parts of southern Africa (excluding the southern tip), and over most of northern South America. Reduced precipitation occurred over parts of southern Brazil and northern Argentina. While the La Niña pattern emerged over parts of the globe, over the contiguous southern United States, the expected drier-than-average pattern did not materialize (with the exception of Florida) and instead the pattern was largely average or wetter-than-average.

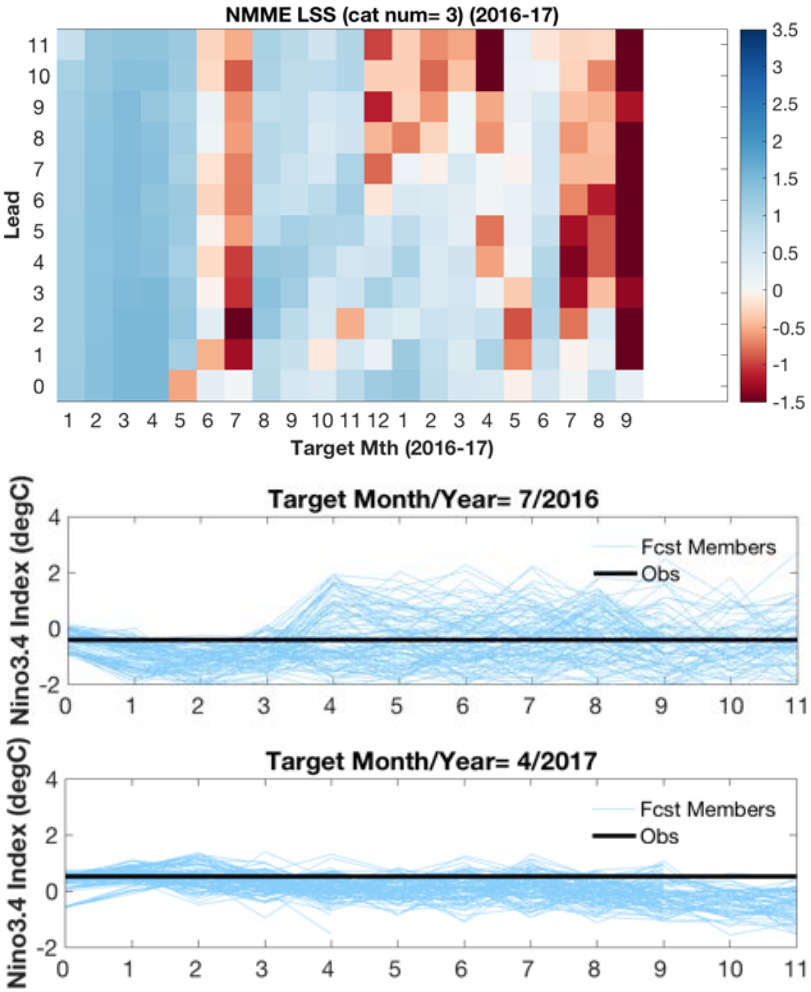

Fig. 2 (top panel) The Logarithmic Skill Score (LSS) of the Niño-3.4 index for target months between January 2016 and September 2017 out to 12-months lead from the NMME (more info on LSS in Tippett *et al.*, 2017). Red shading indicates skill that is worse than climatological forecasts and blue shading indicates skill better than climatological forecasts. Also shown are the forecasts of Niño-3.4 for all ~100 members from the NMME (blue lines) for targets of July 2016 (middle panel) and for April 2017 (bottom panel). The horizontal black line shows the observed Niño-3.4 index value for that target month. On the x-axis is the lead time in months.

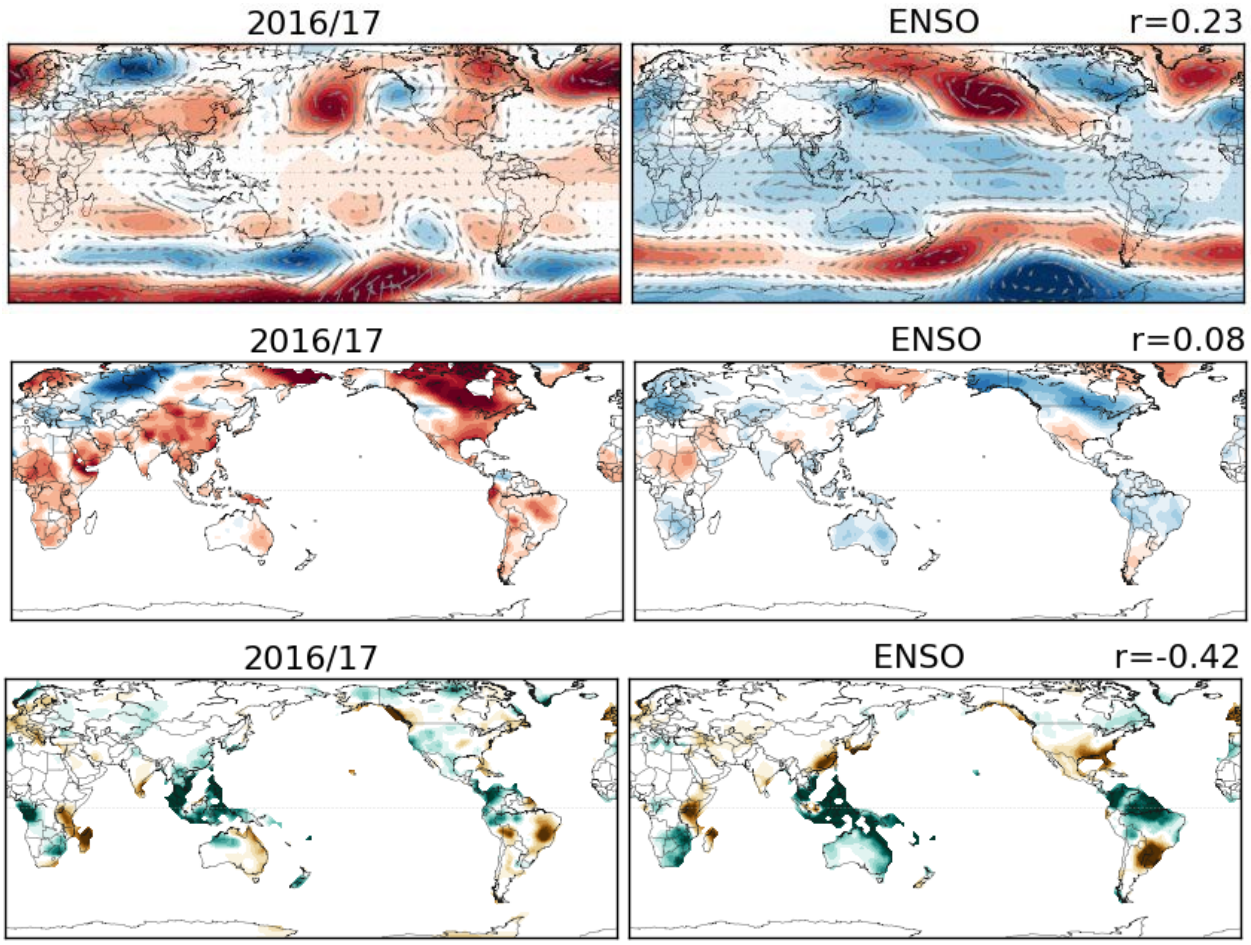

Fig. 3 November 2016-January 2017 (NDJ) anomalies of 500-hPa geopotential height and winds (top row), surface temperature (middle row), and precipitation (bottom row). The left column shows the observational data, while the right column shows the reconstruction for 2016-17 (weighted regression map of the Niño-3.4 index). The reconstruction is multiplied by a factor of eight to aid comparison. The r-values show the spatial correlation coefficient between the observational and the reconstructed anomalies (cosine weighted by latitude). Geopotential height and wind data is from the NCEP/NCAR Reanalysis, the temperature is from the gridded GHCN+CAMS dataset (Fan and van den Dool, 2008), and precipitation data is from the gridded Precipitation Reconstruction Dataset (PREC) dataset (Chen *et al.*, 2002). Departures are formed by removing monthly means during 1981-2010.

Figure 4 shows scatterplots between the Niño-3.4 index values and the NDJ 2016-17 spatial correlations (red dot) relative to other NDJ seasons between 1979-2016 (black dots) for 500-hPa geopotential height (left panel), surface temperature (middle panel), and precipitation (right panel). At the top of each panel in Fig. 4, the temporal correlation is provided between the Niño-3.4 index value and the spatial correlations (between the observed maps and the ENSO regression). From this analysis, it is clear that precipitation and 500-hPa heights have the strongest linkage with Niño-3.4 (r is ~0.9), meaning that larger values of Niño-3.4 are generally associated with larger spatial correlations. Phrased another way, the similarity between the observed global anomalies and the "expected" ENSO pattern is higher with stronger ENSO events. That NDJ 2016-17 was a marginal La Niña with index values closer to -0.5, it follows that the spatial correlations indicated in Fig. 3 are not particularly high.

In fact, one interesting aspect of the NDJ 2016-17 anomalies was how dissimilar the 500-hPa heights were from the ENSO regression (Fig. 3 - top two panels and Figure 4 - left panel). The spatial correlations were positive (r=0.23), meaning the anomalous height pattern was mostly opposite of what would be expected during La Niña. In particular, the global tropics during NDJ 2016-17 were remarkable for its above-average

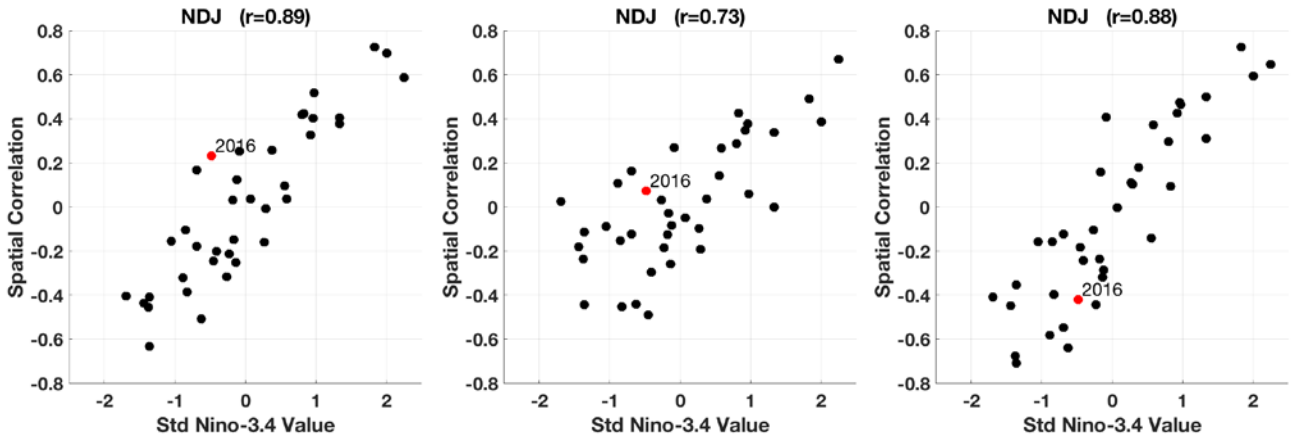

Fig. 4 Scatterplots of the spatial correlation between the ENSO regression maps of 500mb geopoential height (left panel), temperature (middle panel) and precipitation (right panel) and the observed anomalies. The spatial correlation coefficient is on the y-axis and the seasonal average Nino-3.4 index value is on the x-axis. Each dot represents a single year between 1982-2017. The red dot indicates the 2016-17 La Niña (the spatial correlations are also presented in Fig. 3). At the top of each panel are the temporal correlations between the Niño-3.4 values (x-axis) and the spatial correlations (y-axis). The spatial mean is removed.

heights, which are typically below average during La Niña. Also, in the Southern Hemisphere mid-to-high latitudes, the circulation anomalies were reflective of a negative state of the Southern Annular Mode or Antarctic Oscillation, which is usually positive during La Niña. Only over the North Pacific Ocean did an anomalous anticyclone emerge, which is consistent with a retracted Asian jet stream, a common signal during La Niña. The poor fit of the circulation pattern during NDJ 2016-17 has some parallels with other marginal La Niña events (see the black dots surrounding the red dot in Fig. 4- left), but it was certainly striking.

Finally, the correspondence between the expected surface temperature pattern and the observations were very close to zero (r=0.08), indicating little fit between the two. This is evident by the large areas of above-average temperature anomalies that are not commonly seen during La Niña, when below-average temperatures tend to prevail over the globe (Fig. 3- middle row). However, Fig. 4 (middle panel) clearly shows that a weak correspondence between the observations and ENSO regression is often the case during a weak La Niña such as the one that occurred in 2016-17.

Acknowledgements. The ENSO forecast team: Anthony Barnston, Emily Becker, Gerry Bell, Tom Di Liberto, Jon Gottschalck, Mike Halpert, Zeng-Zhen Hu, Nathaniel Johnson, Wanqiu Wang, Yan Xue.

References

Chen, M., P. Xie, J. E. Janowiak, and P. A. Arkin, 2002: Global land precipitation: A 50-yr monthly analysis based on gauge observations. *J. Hydrometeor*., **3**, 249–266.

Fan, Y., and H. van den Dool, 2008: A global monthly land surface air temperature analysis for 1948-present. *J. Geophys. Res.: Atmos.*, **113**, D01103, doi:10.1029/2007JD008470.

Huang, B., and Co-authors, 2017: Extended reconstructed sea surface temperature, version 5 (ERSSTv5): Upgrades, validations, and intercomparisons. *J. Climate*, **30**, 8179–8205.

L'Heureux, M.L., and Co-authors, 2017: Observing and predicting the 2015/16 El Niño. *Bull. Amer. Meteor. Soc.*, **98**, 1363–1382.

Reynolds, R. W., T. M. Smith, C. Liu, D. B. Chelton, K. S. Casey, and M. G. Schlax, 2007: Daily high-resolution-blended analyses for sea surface temperature. *J. Climate*, **20**, 5473–5496.

Tippett, M.K., M. Ranganathan, M. L'Heureux, A. Barnston, and T. DelSole, 2017: Assessing probabilistic predictions of ENSO phase and intensity from the North American Multimodel Ensemble. *Clim Dyn.* https://doi.org/10.1007/s00382-017-3721-y.